Eur. Phys. J. B **34**, 173–177 (2003)
DOI: 10.1140/epjb/e2003-00209-1

THE EUROPEAN PHYSICAL JOURNAL B

Continuous melting of a driven two-dimensional flux lattice with strong pins

L. Fruchter[a]

Laboratoire de Physique des Solides, CNRS, Université Paris-Sud, bâtiment 510, 91405 Orsay Cedex, France

Received 21 March 2003 / Received in final form 27 May 2003
Published online 4 August 2003 –

Abstract. The phase diagram of a driven two-dimensional vortex lattice in the presence of dense quasi-point pins is investigated. The transition from the crystal to the liquid is found continuous at intermediate inductions. The correlations in the pseudo random force that allow for an uncomplete unbinding of the dislocations is proposed as a key mechanism to account for the continuous transition.

PACS. 64.60.Ht Dynamic critical phenomena – 74.60.Ge Flux pinning, flux creep and flux-line lattice dynamics

1 Introduction

It has long been noticed that a driven elastic lattice driven at zero temperature may experience pinning as an effective shaking temperature, due to randomly induced displacements of the lattice nodes. This powerful analogy allows for the prediction of some properties of the driven lattice from the common phase diagram of particles with a repulsive interaction. In particular, a dynamic melting transition is predicted and observed numerically [1]. However, strongly disordered systems, as obtained in the presence of strong quasi-point pins, may move aside from this picture. Indeed, the thermal analogy may break down for the moving crystal due to temporal correlations of the pseudo thermal Langevin force, a situation which is encountered in the case of heterogeneous pinning involving plastic flow channels [2]. As a consequence, while this analogy accounts for the existence of a first order-like dynamic transition, the driven phases may differ from their thermodynamic analogues. Several examples of such exotic phases have been given in references [3–6]. The anisotropy of the pinning potential, once tilted by the external force, is essential to the formation of these phases [2,7]. Here, the dynamic transition is examined in detail for a simple system of dense quasi-point pins with positional disorder. For part of the phase diagram, it is found that there is a continuous transition between the crystal and the liquid, through what might be called a liquid crystal, whereas the transition is first order like for the rest of the phase diagram. In the case of the continuous transition, disclinations tend to form chains, which likely arise from the correlations of the pseudo random force which are specific to the driven lattice.

[a] e-mail: fruchter@lps.u-psud.fr

2 Experiment

The numerical sample used here is the one in reference [8]. It is the one of two dimensional particles with a repulsive interaction, interacting also with a random attractive potential. The sample mimics a two dimensional vortex lattice, or a three dimensional rigid vortex lattice, in the presence of strong pins, as can be created by heavy ions irradiation. Adopting the terminology of superconductors, the vortex density is set by the magnetic induction, B, as $n = a_0^{-2} = B/\Phi_0$ - Φ_0 being the flux quantum carried by each vortex (2×10^{-7} G cm^2). The repulsive force between vortices is taken as:

$$f_{vv}(r) = (A_V/\lambda)\, K_1\,(r/\lambda) \tag{1}$$

where K_1 is a Bessel function, behaving as ln r^{-1} at short distance and $r^{-1/2}\exp(-r)$ at large distance. To keep computation tractable, the repulsive force is cut smoothly at a distance $11a_0$, which insures that each particle interacts with many of its closest neighbors.

The short range potential originates from strong pins randomly distributed in the sample, each creating the attractive force in the range r_P:

$$f_p(r) = (2\ A_P/r_P)\ (r/r_P), \text{ for } r \le r_P;\ 0 \text{ for } r > r_P. \tag{2}$$

All pins are identical and the randomness of the potential originates from the pins position only.

In the rest, driving current densities are normalized to the single vortex critical current density, $J_c = 2\ A_P/r_P\ \Phi_0$. The density of the pinning sites, relative to that of the vortices, B_Φ/B, is constant and equal to 12. The pinning potential range, relative to the vortex average separation, is also constant and equal to

$r_P/a_0 = 5.5 \times 10^{-2}$, as well as the reduced force magnitude, $\lambda A_P/r_P A_V = 20$. As a consequence, using a_0 as the length scale, the different numerical experiments made for different values of the induction B only differ by the reduced vortex interaction length, λ/a_0, where it was set $\lambda = 1400$ Å. As in [8], the total force on each vortex, originating from its neighbors, a possible pinning site at the vortex location and the uniform external force is computed at each time step. Vortices which are not pinned are then moved on a time interval small enough so that their motion is small compared to all characteristic lengths. The boundary conditions are periodic along the driving force direction. A large area free from any pinning site is kept at the sample edges parallel to the vortex motion, where a perfect hexagonal lattice is obtained under the action of the external magnetic pressure [8]. In this way, the measurements actually sample the driven phase embbeded in the crystal. Whereas such an interface may promote the formation of the ordered phase in the case of a first order transition and for finite samples, in the case of a continuous transition, as will be discussed later, the interface probably induces an interfacial layer only. In the following, samples far enough from the interface are considered and their uniformity is an indication that finite size effects are not playing a major role when a continuous transition is observed.

Experiments are carried out for different values of the induction and of the external force. After a stationary state is obtained (characterized by a steady average velocity), a snapshot of the moving lattice is recorded, on which a Delaunay triangulation is performed. Positive and negative disclinations (vortices with coordinance 5 and 7), either free or forming dislocations by pairs [9] are counted. Samples typically enclose 7000 vortices and 4×10^4 pins.

3 Results and discussion

As shown in reference [8], as the driving force decreases, the system evolves from a moving crystal to an amorphous phase. Contrasting with the results in [3–5], the high velocity phase does not show here smectic ordering, as evidenced from the diffraction pattern: this comes from the small ratio r_p/a_0 and from the fact that the tilted pinning potential shows here a moderate anisotropy on the scale of a_0. There is no attractive interaction between the vortices, which would allow for a transition between a liquid and a gas. However, considering the comparable densities of the crystal and the less ordered phase, as well as the strong interactions between the vortices in the amorphous phase, it must obviously be called a 'liquid phase'. As evidenced in Figures 1 and 2 and the inspection of the average hexatic parameter, $|\langle \Psi_6 \rangle| = |\langle 1/c_\alpha \sum_{\beta=1,c_\alpha} \mathrm{e}^{6\,i\,\theta_{\alpha,\beta}} \rangle_\alpha|$ where is c_α the coordination number for vortex α and $\theta_{\alpha,\beta}$ is the angle of the bond between neighboring vortices α and β, some residual orientational correlation is retained for low j ($|\langle \Psi_6 \rangle| \simeq 0.1$), which justifies to call the low j phase an 'hexatic liquid' [4].

I now examine in more detail the transition between the crystal and the liquid. For all systems, the concentration of defects exhibits a clear onset upon decreasing the driving force, similar to the one reported in [1]. However, depending on the magnetic pressure, a discontinuous or gradual rise of this concentration is observed. This may be seen in Figures 1 and 2 obtained for two different magnetic inductions, which clearly exhibit respectively a gradual and a step increase of the number of defects. In order to quantify this observation, the defects concentration was fitted with an exponential, $n_d \propto 1 - \exp[(j_o - j)/\delta]$ ($j < j_o$), yielding the onset, j_o, and a width for the transition to the liquid phase, δ. A phase diagram similar to the temperature-density representation for the thermodynamics may be obtained, using the theory for the equivalent 'shaking temperature' [1]. It should be stressed that this representation is qualitative only, considering the

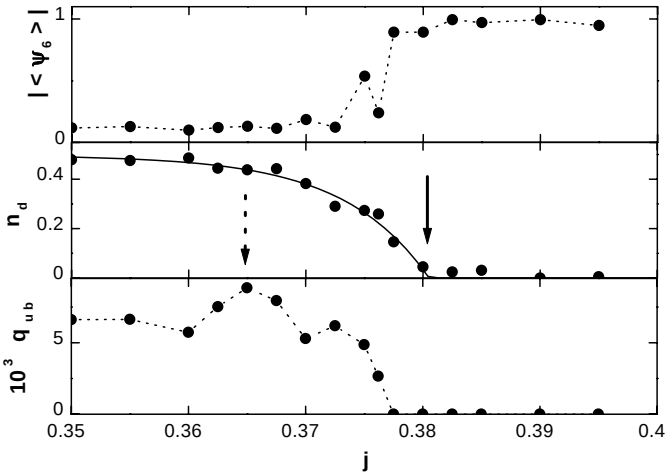

Fig. 1. $B = 3950$ Oe. From top to bottom: Hexatic parameter, concentration of defects (sites with coordination number not equal to 6), concentration of free disclinations (defects bound to sites with coordination number 6 only). The line is the fit described in the text; the full line arrow indicates the onset for the defects creation, as obtained from this fit; the dotted one is the melting point as obtained in Figure 6.

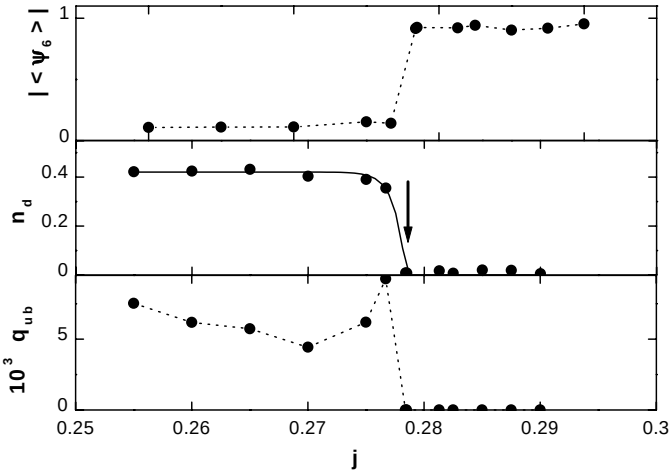

Fig. 2. $B = 10^4$ Oe.

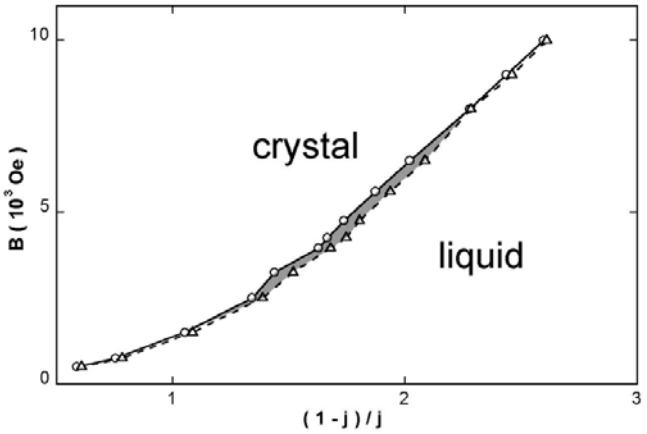

Fig. 3. Dynamic phase diagram of the driven lattice. Circles: $j = j_o$, triangles: $j = j_o - \delta$.

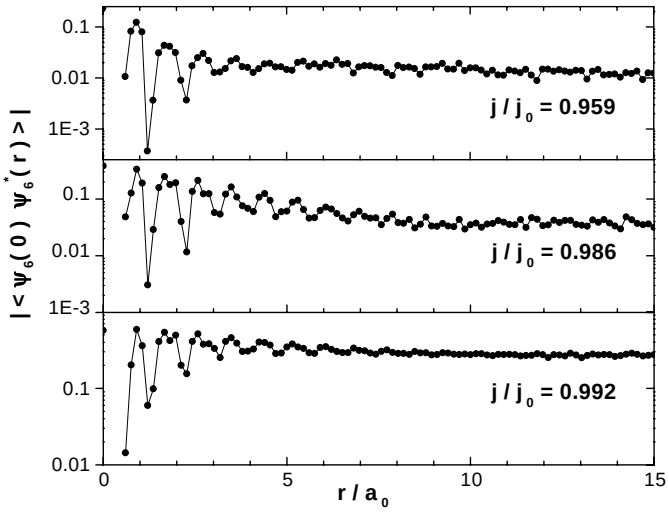

Fig. 4. The correlation function for the hexatic parameter. ($B = 3950$ Oe).

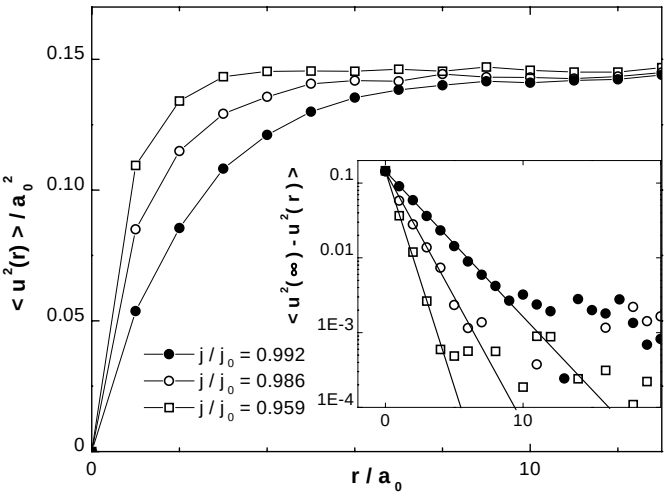

Fig. 5. The correlation function for the displacement field. ($B = 3950$ Oe).

reservations made in references [1,2] (mainly, the perturbative approach from the uniform velocity which rules out plasticity, and the observation that the effective temperature differs for the fluidlike motion and the coherent one). Also, the equivalent temperature in [1], must be modified to account for the proximity of the flux flow to the flux creep crossover. Imposing for the equivalent temperature to be proportional to the potential well depth when $j_o \to 1$ and $B \to 0$, $T \propto (1-j)$, and using $T \propto j^{-1}$ from [1], a phase diagram is obtained in the B *vs.* $(1-j)/j$ representation. The onset for the defects concentration (j_o), as well as the location where it saturates ($j_o - \delta$), are plotted in this way in Figure 3. Clearly, there is a range of magnetic induction for which a regime, intermediate between the moving crystal and the hexatic liquid, can be found. The existence of such a regime was already pointed out in [8].

In order to characterize the continuous transition, let us examine some autocorrelation functions which are classical tools for the study of solids and liquids. The average hexatic order parameter does not provide an accurate characterization of the intermediate regime: as may be seen in Figure 1, following a sharp drop at $j = j_o$, there is no significative change at lower j where the density of defects however still exhibits significant variations. The *spatial correlations* of the hexatic parameter carry more useful information [9]. The correlator $\langle \Psi_6(0)\ \Psi_6^*(r)\rangle_r$ for the data in Figure 1 is shown in Figure 4. Besides the existence of a non zero background related to the non zero averaged value $|\langle \Psi_6 \rangle|$, it reveals some additional short range correlations of the orientational order, which extends to a larger range as the system is closer to j_o. The oscillations for small r reflect the existence of a crystalline order within this range: they are associated with the fluctuations of the density autocorrelation function which come with the translational symmetry breaking of the crystal order. This is confirmed by the examination of the growth of the displacement field (actually a positional correlation function): $\langle \mathbf{u}^2(r = n\ a_0)\rangle = \langle \sum_j \mathbf{u}^2(n\ [\mathbf{r}_j - \mathbf{r}_i])\rangle_i$ where j denotes one of the nearest neighbors of vortex i in a Delaunay triangulation and $\mathbf{u}$ is the displacement field from the periodic arrangement. As may be seen in Figure 5, there is an exponential decay of the positional correlations, with a diverging correlation length, $\xi(j)$, as one approaches j_0 from below (*i.e.* from larger 'temperatures'). Following reference [9], one may then call this regime an 'hexatic liquid crystal'. It is possible to track the positional correlation length in Figure 5 as one approaches j_0. The result is diplayed in Figure 6 showing a divergence as $\xi = \xi_0\ (1 - j/j_0)^{-1}$, with the bare correlation length $\xi_0 \simeq 0.15\ a_0$. Recalling the Lindeman melting criterion, $\langle u^2 \rangle = c_L^2\ a_0^2$ and the exponential increase of the displacement field, $\langle u^2 \rangle = \langle u^2(\infty)\rangle(1 - \exp(-r/\xi))$, one may write an equivalent melting criterion for the present case as $a_0/\xi = \ln(1 - c_L^2\ a_0^2/\langle u^2(\infty)\rangle)$. The result obtained using $c_L \approx 0.2$ and $\langle u^2(\infty)\rangle \simeq 0.14$, $a_0/\xi \approx 0.3$, is displayed in Figures 1 and 6. Although this quantitative result should be considered with caution, due to the

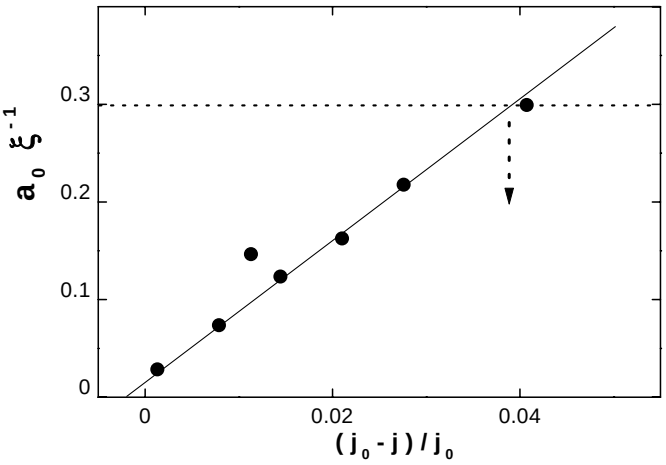

Fig. 6. $B = 3950$ Oe. Correlation length for the positional order, as obtained from the data in Figure 5. The full line is a linear fit. The dotted line represents $\langle u^2 \rangle = c_L^2\ a_0$ with $c_L = 0.2$. The melting point, as indicated by the dotted arrow, is shown in Figure 1 also.

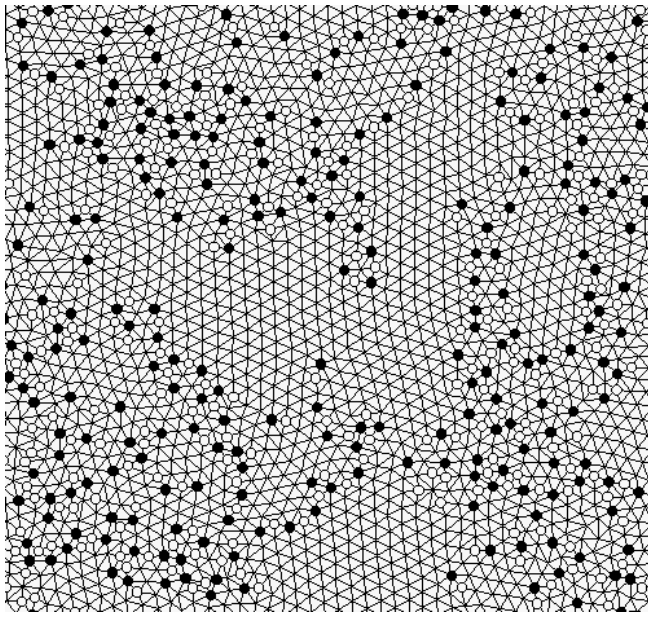

Fig. 7. Positive - five-coordinated (white) and negative - seven-coordinated (black) disclinations in a sample driven along the vertical axis. ($B = 3950$ Oe, $j = 0.375$).

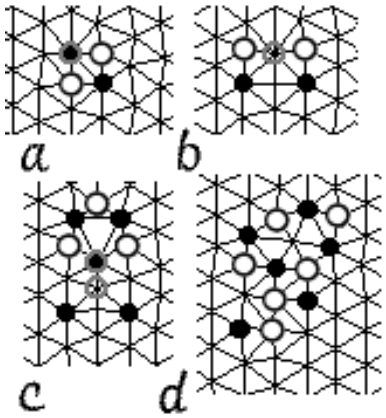

Fig. 8. Early steps for the creation of defects ($B = 3950$ Oe, $j = 0.375$. Nodes of the Delaunay triangulation lines are vortices. Filled and opened circles are disclinations as in Fig. 7; gray circles indicate vortices which are located in a potential minimum). Configurations a) and b) are obtained consecutively as the result of the trapping of one vortex. Configuration c) and d) are later steps. Vortices are driven to the top of the figure.

uncertainty on the effective Lindeman number, this confirms that the solid has not melted in the conventional way below the threshold value j_0.

The observation that the transition is continuous at intermediate induction and involves a proliferation of defects appeals for a comparison with the KTHNY extension of the Kosterliz-Thouless theory [9,10]. The theory of dislocation mediated melting of two-dimensional solids accounts for a continuous transition, involving first unbinding of the dislocations leading to the hexatic liquid, and then unbinding of the disclinations leading to the regular liquid. Here, dislocations do not first dissociate at j_0 to form an homogeneous 'plasma'. Rather, they tend to form chains of alternating positive (five-coordinated) and negative (seven-coordinated) disclinations which proliferate in the liquid phase. As a result, unbounded dislocations and disclinations remain marginal (Fig. 7). Correlations between dislocations were also reported in reference [4] where free dislocations, although not bound in chains, formed quenched patterns moving with the average flux flow. In order to explain the formation of these chains, the examination of the early creation of defects in a driven crystal may be useful. Snapshots of the earlier defects detected in a sample driven in the intermediate region in Figure 1 are displayed in Figure 8. After a dislocation pair with opposite Burger vectors has been created by the pinning of one vortex (a), it is seen that the dislocations quickly arrange to form rings of diameter $\sim 2\ a_0$ (c) and then larger loops (d). Remarkably, the composite defects reflect the external force anisotropy as soon as the dislocations dissociate (b): this results from the plastic mechanism at work to create these defects. This is also a direct evidence that the correlations in the pseudo random force cannot be neglected in their formation. The relation between these initial stages and the formation of chains is not completely clear. A possible mechanism is the stretching of elementary loops as in Figure 8d, as the vortices making disclinations appear to become more easily pinned than the regular ones. This would make the long-range 'random force' correlations a key ingredient in the chain formation again. Equivalent rates for the growth and the annihilation of the chains would then account for the existence of a stationary regime intermediate between the crystal and the liquid.

In conclusion, it is found that a vortex lattice driven on dense quasi-point pins shows a continuous transition between the crystal and the liquid at intermediate induction, while first order otherwise. The binding of the disclinations in chains is proposed as a key mechanism to account for the existence of the continuous transition.

Simulations have been performed on the cluster of the "Centre de Ressources Informatiques de l'Université Paris-Sud (CRI)".

References

1. A.E. Koshelev, V.M. Vinokur, Phys. Rev. Lett. **73**, 3580 (1994)
2. L. Balents, M.C. Marchetti, L. Radzihovsky, Phys. Rev. B **57**, 7705 (1998)
3. K. Moon, R.T. Scalettar, G.T. Zimanyl, Phys. Rev. Lett. **77**, 2778 (1996)
4. R. Seungoh, M. Hellerqvist, S. Doniach, A. Kapitulnik, D. Stroud, Phys. Rev. Lett. **77**, 5114 (1996)
5. C.J. Olson, C. Reichhardt, F. Nori, Phys. Rev. Lett. **81**, 3757 (1998)
6. H. Fangohr, S.J. Cox, P.A.J. de Groot, Phys. Rev. B **64**, 064505 (2001)
7. P. Le Doussal, T. Giamarchi, Phys. Rev. B **57**, 11356 (1998)
8. L. Fruchter, Eur. Phys. J. B **25**, 313 (2002)
9. D.R. Nelson, B.I. Halperin, Phys. Rev. B **19**, 2457 (1979)
10. A.P. Young, Phys. Rev. B **19**, 1855 (1979)